

APPLICATIONS OF PProDOT-Bz₂/PT COMPOSITE COUNTER ELECTRODES IN DSSCS UNDER DIFFERENT ILLUMINATION INTENSITIES

Tzi-Yi Wu¹, Yu-Chi Huang², Jung-Chuan Chou^{3*}, Yu-Hsun Nien¹, Chih-Hsien Lai⁴, Po-Yu Kuo⁵, Yi-Hung Liao⁶, Cheng-Chu Ko⁷, and Jun-Xiang Chang⁷

ABSTRACT

Poly(3,3-dibenzyl-3,4-dihydro-2H-thieno[3,4-b][1,4]dioxepine) (PProDOT-Bz₂)/platinum (Pt) composites films were employed as counter electrodes (CE) for dye-sensitized solar cells (DSSCs). The composite films were deposited onto fluorine-doped tin oxide (FTO) substrate by sputtering Pt for 10 s and 30 s (Pt-FTO glass). 25 mC cm⁻² and 50 mC cm⁻² PProDOT-Bz₂ were electrochemically synthesized on 10 s and 30 s Pt-FTO glass. The composites films were characterized via electrochemical impedance spectroscopy (EIS). The DSSC based on 25 mC cm⁻² PProDOT-Bz₂/30 s Pt composite films exhibits short-circuit current density (J_{sc}) of 11.11 mA cm⁻², open circuit voltage (V_{oc}) of 0.62 V, fill factor (FF) of 68.74%, and the photovoltaic conversion efficiency of 4.72%. Furthermore, the DSSC is a promising device because it can work under indoor fluorescent light. In this study, the composites counter electrodes under different light intensities are also investigated.

Keywords: Electrosynthesis, counter electrode, light intensity, PProDOT-Bz₂.

1. INTRODUCTION

Dye-sensitized solar cells (DSSCs) have become increasingly attractive due to their low cost and easy fabrication, after the report revealed by O'Regan and Grätzel in 1991 (O'Regan and Grätzel 1991). The CE of DSSCs is part of an important component in DSSCs. Meanwhile, Pt has superior electrochemical catalytic activity, good corrosion resistance, small resistance, large electrochemical active area and high reflecting properties, and so it has been regarded as suitable CE material. However, platinum-based CE is too expensive to be applied to DSSCs. With this in mind, research into this has been conducted to explore several possible substitutes. This is to substitute the CE material for platinum in DSSCs. Carbon-based materials, such as graphite, carbon black (Kay and Grätzel 1996; Liu *et al.* 2016), carbon nanotubes (CNTs)

Manuscript received December 4, 2019; revised March 3, 2020; accepted March 16, 2020.

¹ Professor, Dept. of Chemical and Materials Eng., National Yunlin University of Science and Technology, Douliou, Yunlin, Taiwan 64002, R.O.C.

² Master student, Dept. of Chemical and Materials Eng., National Yunlin University of Science and Technology, Douliou, Yunlin, Taiwan 64002, R.O.C.

^{3*} Chair Professor (corresponding author), Dept. of Electronic Eng., National Yunlin University of Science and Technology, Douliu, Taiwan 64002, R.O.C. (e-mail: choujc@yuntech.edu.tw)

⁴ Professor, Dept. of Electronic Eng., National Yunlin University of Science and Technology, Douliu, Taiwan 64002, R.O.C.

⁵ Assistant Professor, Dept. of Electronic Eng., National Yunlin University of Science and Technology, Douliu, Taiwan 64002, R.O.C.

⁶ Associate Professor, Dept. of Information and Electronic Commerce Management, TransWorld University, Douliou, Taiwan 64002, R.O.C.

⁷ Master student, Dept. of Electronic Eng., National Yunlin University of Science and Technology, Douliou, Taiwan 64002, R.O.C.

(Vijayakumar *et al.* 2017), carbon nanorods (CNRs) (Wang *et al.* 2017), hard carbon spheres (Bu and Kao 2017), graphene (Ma *et al.* 2017; Ghasemi *et al.* 2017; Zhou *et al.* 2016; Nemala *et al.* 2017; Kavan *et al.* 2016; Yuan *et al.* 2017; Miao *et al.* 2017) and carbon material fabricated from sucrose and glucose, etc., are considered to have great potential to replace Pt as counter electrode in recent years. They are low-cost and exist in large numbers. Also they have high catalytic activity and remain good chemical stability (Kang *et al.* 2016; Kumar *et al.* 2017). More importantly, conducting polymers are suitable to replace Pt as CEs due to their low-cost, excellent catalytic activity, and good conductivity. These properties are believed to have great potential to fabricate large-area CEs. In the past few years, conducting polymers, e.g. polyaniline (PANI)(Li *et al.* 2008; Li *et al.* 2009; Zhang *et al.* 2010), polypyrrole (PPy)(Bu *et al.* 2013; Veerender *et al.* 2012; Towannang *et al.* 2012), poly-3-methyl-thiophene (P3HT)(Torabi *et al.* 2014), poly (3,4-ethyl-enedioxythiophene)(PEDOT) (Belekoukia *et al.* 2016; Li *et al.* 2017; Kim *et al.* 2016), PEDOT:PSS (Li *et al.* 2013; Yue *et al.* 2015) and 3,4-propylenedioxythiophene derivatives (PProDOT derivatives) (Yeh *et al.* 2011) have been reported as promising CEs of DSSCs. Among them, PP or DOT derivatives have good catalytic properties and high specific surface areas. M.H. Yeh *et al.* have prepared PProDOT-Et₂/10 s Pt as CEs. The power conversion efficiency of DSSCs with the PProDOT-Et₂/10 s CE is 6.65%, which is higher than that of Pt CE with sputtering time for 720 s (6.43%)(Yeh *et al.* 2011). The improvement of photoelectric conversion efficiency for PProDOT- Et₂/Pt-based CE was ascribed to PProDOT-Et₂, for this showed a markedly high electrochemical surface area for the reduction from I³⁻ to I⁻(Yeh *et al.* 2011). In this study, we synthesized a novel polymer of PProDOT-Bz₂ electrochemically and prepared the PProDOT-Bz₂/Pt composite film, by combining Pt with different sputtering time and PProDOT-Bz₂ with different charge capacity to improve the photoelectric conversion efficiency.

2. EXPERIMENTAL

2.1 Materials

TiO_2 paste (ETERDSC Ti-2105) and (ETERDSC Ti-2325) were provided by Eternal Materials Co., Ltd., Taiwan. Ruthenium-535 (N3), iodine (I_2), lithium iodide (LiI), 4-tert-butylpyridine (TBP), absolute ethanol, and 1-propyl-2,3-dimethylimidazolium iodide were ordered from TCI company, UniRegion Bio-Tech, Katayama Chemical, Sigma-Aldrich, and Riedel-deHaen, and they were used as received. FTO substrates were obtained from C.P. Solar, Co., Ltd.

2.2 Synthetic procedure of ProDOT-Bz₂ monomer

1 g (0.007 mol) of 3,4-dimethoxythiophene, 1.37 g (0.0054 mol) of 2,2-dibenzyl-1,3-propanediol, 0.04 g (0.0002 mol) of p-toluenesulfonic acid, and 50 mL of toluene, were combined in a round-bottomed flask. The solution was heated at 110°C under nitrogen for 2 days. The product was purified by flash column chromatograph along with silica gel used as stationary phase and dichloromethane/hexane (volume ratio of 1:2) used as the mobile phase. ProDOT-Bz₂ was a white powder and the yield was 60%. ¹H NMR (700 MHz, CDCl_3 , ppm): δ 7.27 (m, 10H, phenyl-H), δ 6.49 (s, 2H, Th-H), δ 3.85 (s, 4H, OCH₂-), δ 2.85 (s, 4H, phenyl-CH₂-).

2.3 Fabrication of PProDOT-Bz₂ counter electrodes

Figure 1 (a) provides schematic procedures of the preparation of PProDOT-Bz₂/Pt composite counter electrode. The FTO glasses were sequentially cleaned via sonication in acetone, ethanol, and D. I. water. The various Pt-FTO substrates were fabricated by sputtering Pt for 10s and 30 s onto FTO glass. The sputtering parameters of Ar flow rate, working pressure, and ration frequency sputtering power kept 10 sccm, 30 mTorr, and 60 W. The electrochemical system was mainly comprised of three electrodes, including various Pt-FTO glass substrates as working electrodes, Pt wires as counter electrodes, and Ag/AgCl as reference electrodes. The PProDOT-Bz₂ films were electro synthesized by potentiostatically at the potential of 1.4 V on Pt-FTO glass substrates using 0.1 M LiClO_4 and 6 mM ProDOT-Bz₂ in CH_3CN solution. The charge density was fixed at 25 or 50 mC cm^{-2} , respectively. Then, the prepared films were heated at 70°C for 1 h to remove the solvent.

2.4 Assembly of the DSSCs

The 12 μm double-layer TiO_2 film was comprised of a transparent layer with a thickness of 8 μm (ETERDSC Ti-2105), combined with a light scattering layer with a thickness of 4 μm (ETERDSC Ti-2325) being coated in the cleaned FTO substrates by using the doctor blade method. Each layer was sintered in air at 500°C for 30 min. After sintering, the photoanode was immersed into the dye solution containing 0.3 mM N3 dye in ethanol for one day at room temperature. Finally, the TiO_2 photoanodes were coupled with various counter electrodes and electrolyte by a sandwiching process. The electrolyte solution was observed to contain 0.5 M lithium iodide, 0.05 M iodide, 0.5 M 4-tert-butylpyridine (TBP) and 0.6 M 1-propyl-2,3-dimethylimidazolium iodide (DMPII) in 3-methoxypropionitrile/acetonitrile (volume ratio of 1:1). The active area of the DSSCs was 0.25 cm^2 . The components of the DSSCs are shown in Fig. 1 (b).

3. RESULTS AND DISCUSSION

3.1 Photovoltaic performances

The J-V curves of DSSCs based on different CEs under 100 mW cm^{-2} light illumination are presented in Fig. 2, and the photovoltaic parameters are summarized in Table 1. As shown in Table 1, it could be described that DSSC based on PProDor-Bz₂/Pt composites CEs had a slightly lower V_{oc} than that of pure Pt CEs. The V_{oc} of DSSC depended on the discrepancy between the quasi-Fermi level of the electrons in the TiO_2 layer and the oxidation and reduction potentials of electrolyte. In this case, DSSCs were constructed by identical photoanode structures and electrolyte but with various CEs. Therefore, the different V_{oc} can be ascribed to the slightly poor electrocatalytic activity of PProDor-Bz₂/Pt composites CEs. The higher PProDor-Bz₂ concentration of CEs surface exhibited lower V_{oc} (Bora *et al.* 2015). However, from Table 1, it could be also demonstrated that the PProDor-Bz₂/Pt composites CEs had higher J_{sc} than that of Pt CEs, which is due to its porous structures. The 25 mC cm^{-2} PProDOT-Bz₂/10 s Pt and 25 mC cm^{-2} PProDOT-Bz₂/30 s Pt composite counter electrodes provided the η of 3.62% and 4.72%, which were higher than those of 10 s Pt (3.20%) and 30 s Pt (3.77%) CE. The η for them increase 13% and 25%, respectively.

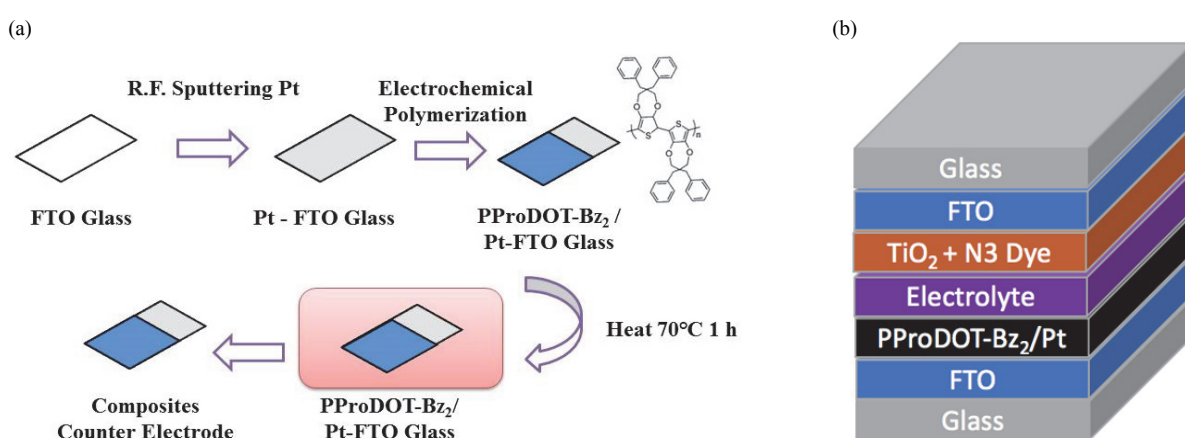
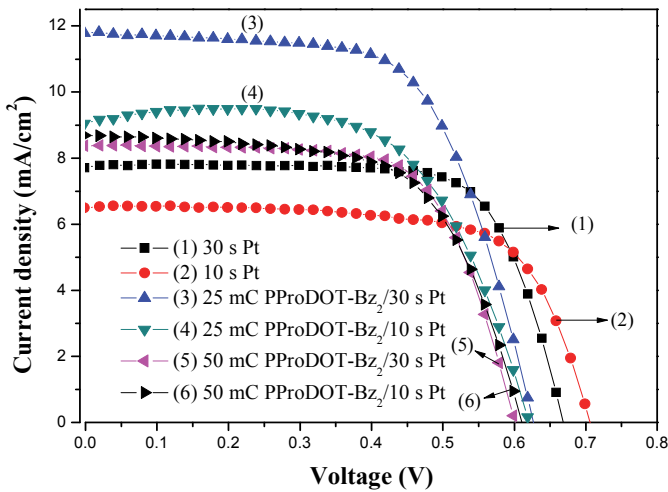


Fig. 1 (a) Schematic procedures of the PProDOT-Bz₂/Pt composite counter electrodes and (b) schematic diagram of DSSCs structure

Table 1 The photovoltaic parameters of the DSSCs with different CEs

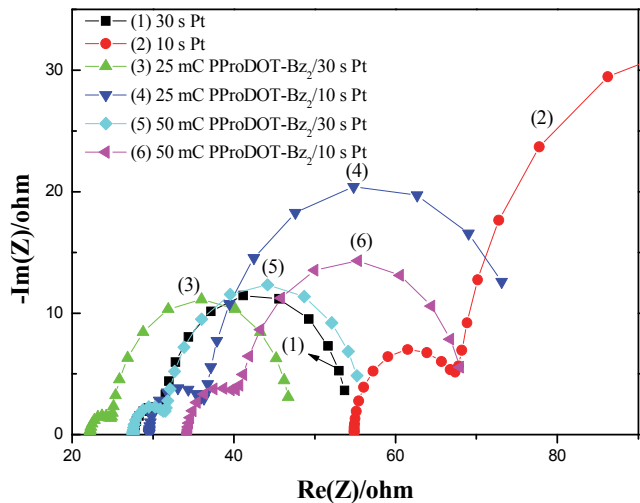
CEs	V _{oc} (V)	J _{sc} (mA/cm ²)	FF	η (%)	Ref.
10s Pt	0.70	6.53	0.70	3.20	In this study
30s Pt	0.66	7.79	0.73	3.77	In this study
25 mC cm ⁻² PProDOTBz ₂ /10 s Pt	0.62	9.17	0.64	3.62	In this study
25 mC cm ⁻² PProDOTBz ₂ /30 s Pt	0.62	11.81	0.65	4.72	In this study
50 mC cm ⁻² PProDOTBz ₂ /10 s Pt	0.60	8.68	0.64	3.33	In this study
50 mC cm ⁻² PProDOTBz ₂ /30 s Pt	0.60	8.38	0.67	3.42	In this study
Pt	0.72	9.50	0.65	4.40	Xia et al. 2011
PPy	0.68	9.20	0.52	3.40	Xia et al. 2011

**Fig. 2** The J-V curves of DSSCs based on different counter electrodes

3.2 Electrochemical impedance spectra

Figure 3 shows the Nyquist plots of the DSSCs based on various counter electrodes. The values of RS, R₁ and R₂ obtained by fitting the Nyquist plots are summarized in Table 2. The RS value could be estimated using the onset point of the first semicircle in the high frequency zone. A lower RS presents a better adherence of the catalytic layer onto the substrate and thereby gives rise to a good electrical conductivity of the film and good fill factor (FF) of DSSC (Chen et al. 2015). The first

semicircle in the high frequency region of EIS indicates the charge transfer resistance (R₁) at the interface between electrolyte and composite CE, which determines electrocatalytic performances of the counter electrode towards I³⁻ reduction (Bora et al. 2015). The second semicircle indicates the charge transfer resistance at the interface of the photoanode and electrolyte (R₂) (Mehmood 2016). The CE based on PProDOT-Bz₂/Pt showed a lower R₁ value than that of Pt CE.

**Fig. 3** The Nyquist plots of the DSSCs based on various counter electrodes**Table 2** The capacitance and resistance of the equivalent circuit for DSSCs able

CEs	R _S (Ω)	C ₁ (μF)	R ₁ (Ω)	C ₂ (mF)	R ₂ (Ω)
10s Pt	54.86	25.82	12.51	0.61	65.03
30s Pt	27.67	82.36	2.98	0.79	23.01
25 mC cm ⁻² PProDOTBz ₂ /10 s Pt	29.54	47.30	6.76	0.97	36.81
25 mC cm ⁻² PProDOTBz ₂ /30 s Pt	22.19	114.97	2.57	1.77	21.96
50 mC cm ⁻² PProDOTBz ₂ /10 s Pt	32.33	71.23	5.91	0.93	27.72
50 mC cm ⁻² PProDOTBz ₂ /30 s Pt	27.52	53.71	3.96	1.08	23.74

3.3 The photovoltaic parameters of the DSSCs with 25 mC cm^{-2} PProDOT-Bz₂/Pt composite counter electrodes at different light intensities

Figure 4 displays the J-V curves of DSSC based on 25 mC cm^{-2} PProDOT-Bz₂/30 s Pt counter electrode at different light intensities. The corresponding photovoltaic parameters are summarized in Table 3. The 25 mC cm^{-2} PProDOT-Bz₂/30 s Pt composite counter electrodes at 100 mW cm^{-2} , 80 mW cm^{-2} , 50 mW cm^{-2} , 30 mW cm^{-2} and 10 mW cm^{-2} provided the η of 4.72%, 4.85%, 5.38%, 5.73% and 3.70%, respectively. However, the η of PProDOT-Bz₂/30 s Pt CE increased with decreasing the light intensity. The improvement in efficiency can be attributed to less diffusion overpotential and less electron recombination of the cell under 80 mW cm^{-2} , 50 mW cm^{-2} and 30 mW cm^{-2} than that of 100 mW cm^{-2} (Lan *et al.* 2012). Moreover, Fig. 5 shows the simulated solar light source spectrum.

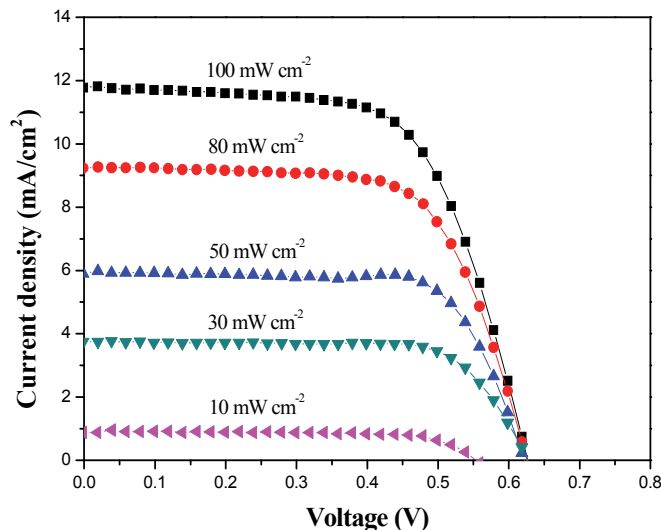


Fig. 4 The J-V curves of the DSSC based on 25 mC cm^{-2} PProDOT-Bz₂/30 s Pt counter electrode at different light intensities

Table 3 The photovoltaic properties of the DSSC with 25 mC cm^{-2} PProDOT-Bz₂/30 s Pt counter electrode at different light intensities

Light intensity (mW cm^{-2})	V_{oc} (V)	J_{sc} (mA/cm^2)	FF	η (%)
100	0.62	11.81	0.65	4.72
80	0.62	9.27	0.68	4.85
50	0.62	5.99	0.73	5.38
30	0.62	3.74	0.74	5.73
10	0.54	0.88	0.78	3.70

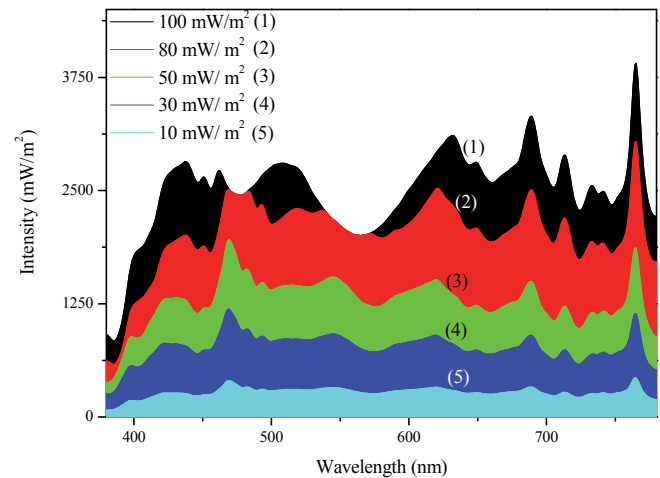


Fig. 5 The spectrum of solar simulator.

4. CONCLUSIONS

This study investigated the impact of various Pt sputtering time of PProDOT-Bz₂/Pt composite counter electrodes and various illumination intensities in DSSCs. The DSSC based on PProDOT-Bz₂/10 s Pt composite counter electrode exhibited a PCE of 3.62%, which is compared with the 30 s Pt CE (3.77%) under the 100 mW cm^{-2} light illumination. The DSSC based on 25 mC cm^{-2} PProDOT-Bz₂/30 s Pt composite films gave the photovoltaic conversion efficiency of 4.72% and 5.73%, under the 100 mW cm^{-2} and 30 mW cm^{-2} light intensities, respectively. From EIS analysis, the PProDOT-Bz₂/Pt composite CEs with smaller charge transfer resistances caused higher J_{sc} and η . Accordingly, the PProDOT-Bz₂/Pt composite CEs are deemed as promising candidates to replace Pt as an inexpensive counter electrodes material in DSSCs. Because the DSSC has better photovoltaic performances under low light intensity, it is important to further investigate the cell performance under low illumination intensity.

ACKNOWLEDGMENTS

This study was supported by the Ministry of Science and Technology (MOST), Taiwan, under the contracts MOST 108-2221-E-224-020 and Most 107-2221-E-224-030.

REFERENCES

- Belekoukia, M., Ramasamy, M.S., Yang, S., Feng, X., Paterakis, G., Dracopoulos, V., Galiotis, C., and Lianos, P. (2016). “Electrochemically exfoliated graphene/PEDOT composite films as efficient Pt-free counter electrode for dye-sensitized solar cells.” *Electrochimica Acta*, **194**, 110-115.
- Bora, C., Sarkar, C., Mohan, K.J., and Dolui, S. (2015). “Polythiophene/graphene composite as a highly efficient platinum-free counter electrode in dye-sensitized solar cells.” *Electrochimica Acta*, **157**, 225-231.

- Bu, C., Tai, Q., Liu, Y., Guo, S., and Zhao, X. (2013). "A transparent and stable polypyrrole counter electrode for dye-sensitized solar cell." *Journal of Power Sources*, **221**, 78-83.
- Bu, I.Y.Y. and Kao, L.Y. (2017). "Flame synthesis of highly graphitic carbon nano-sphere using cobalt-based catalyst." *International Journal of Nanomanufacturing*, **13**, 161-169.
- Chen, P.Y., Li, C.T., Lee, C.P., Vittal, R., and Ho, K.C. (2015). "PEDOT-decorated nitrogen-doped graphene as the transparent composite film for the counter electrode of a dye-sensitized solar cell." *Nano Energy*, **12**, 374-385.
- Ghasemi, S., Hosseini, S.R., and Mousavi, F., (2017). "Electrophoretic deposition of graphene nanosheets: A suitable method for fabrication of silver-graphene counter electrode for dye-sensitized solar cell." *Colloids and Surfaces A: Physicochemical and Engineering Aspects*, **520**, 477-487.
- Kang, G., Choi, J., and Park, T. (2016). "Pt-free counter electrodes with carbon black and 3D network epoxy polymer composites." *Scientific Reports*, **6**, Article number 22987, 9 pages.
- Kavan, L., Liska, P., Zakeeruddin, S.M., and Grätzel, M. (2016). "Low-temperature fabrication of highly-efficient, optically-transparent (FTO-free) graphene cathode for co-mediated dye-sensitized solar cells with acetonitrile-free electrolyte solution." *Electrochimica Acta*, **195**, 34-42.
- Kay, A. and Grätzel, M. (1996). "Low cost photovoltaic modules based on dye sensitized nanocrystalline titanium dioxide and carbon powder." *Solar Energy Materials and Solar Cells*, **44**, 99-117.
- Kim, S.J., Kwon, J., Nam, J.K., Kim, W., and J Park. H. (2016). "Long-term Stability of Conducting Polymers in Iodine/iodide Electrolytes: Beyond Conventional Platinum Catalysts." *Electrochimica Acta*, **227**, 95-100.
- Kumar, R., Nemala, S.S., Mallick, S., and Bhargava, P. (2017). "Synthesis and characterization of carbon based counter electrode for dye sensitized solar cells (DSSCs) using sugar free as a carbon material." *Solar Energy*, **144**, 215-220.
- Lan, J.L., Wei, T.C., Feng, S.P., Wan, C.C., and Cao, G. (2012). "Effects of iodine content in the electrolyte on the charge transfer and power conversion efficiency of dye-sensitized solar cells under low light intensities." *The Journal of Physical Chemistry C*, **116**, 25727-25733.
- Li, C.T., Lee, C.P., Li, Y.Y., Yeh, M.H., and Ho, K.C. (2013). "A composite film of TiS₂/PEDOT:PSS as the electrocatalyst for the counter electrode in dye-sensitized solar cells." *Journal of Materials Chemistry A*, **1**, 14888-14896.
- Li, H., Xiao, Y., Han, G., and Hou, W. (2017). "Honeycomb-like poly(3,4-ethylenedioxythiophene) as an effective and transparent counter electrode in bifacial dye-sensitized solar cells." *Journal of Power Sources*, **342**, 709-716.
- Li, Q., Wu, J., Tang, Q., Lan, Z., Li, P., Lin, J., and Fan, L. (2008). "Application of microporous polyaniline counter electrode for dye-sensitized solar cells." *Electrochemistry Communications*, **10**, 1299-1302.
- Li, Z., Ye, B., Hu, X., Ma, X., Zhang, X., and Deng, Y. (2009). "Facile electropolymerized-PANI as counter electrode for low cost dye-sensitized solar cell." *Electrochemistry Communications*, **11**, 1768-1771.
- Liu, I.P., Hou, Y.C., Li, C.W., and Lee, Y.L. (2016). "Highly electrocatalytic counter electrodes based on carbon black for cobalt(iii)/(ii)-mediated dye-sensitized solar cells." *Journal of Materials Chemistry A*, **5**, 240-249.
- Ma, J., Shen, W., Li, C., Zheng, J., and Yu, F. (2017). "Graphene cryogel-based counter electrode materials freeze-dried using different solution media for dye-sensitized solar cells." *Chemical Engineering Journal*, **319**, 155-162.
- Mehmood, U. (2016). "Efficient and economical dye-sensitized solar cells based on graphene/TiO₂ nanocomposite as a photoanode and graphene as a Pt-free catalyst for counter electrode." *Organic Electronics*, **42**, 187-193.
- Miao, F., Miao, R., Tao, B., Jin, Z., Yu, J., Chu, P.K., Liu, F., Sha, L., Li, C., and Zhu, X. (2017). "Vertically-oriented few-layer graphene supported by silicon microchannel plates as a counter electrode in dye-sensitized solar cells." *Organic Electronics*, **45**, 74-80.
- Nemala, S.S., Kartikay, P., Prathapani, S., Bohm, H.L.M., Bhargava, P., Bohm, S., and Mallick, S. (2017). "Liquid phase high shear exfoliated graphene nanoplatelets as counter electrode material for dye-sensitized solar cells." *Journal of Colloid and Interface Science*, **499**, 9-16.
- O'Regan, B. and Grätzel, M. (1991). "A low-cost, high-efficiency solar cell based on dye-sensitized colloidal TiO₂ films." *Nature*, **353**, 737-740.
- Torabi, N., Behjat, A., and Jafari, F. (2014). "Dye-sensitized solar cells based on porous conjugated polymer counter electrodes." *Thin Solid Films*, **573**, 112-116.
- Towannang, M., Pimanpang, S., Thiangkaew, A., Rutphonsan, P., Maiaugree, W., Harnchana, V., Jarernboon, W., and Amornkitbamrung, V. (2012). "Chemically deposited polypyrrole-nanoparticle counter electrode for inorganic I⁻/I₃⁻ and organic T⁻/T₂ dye-sensitized solar cells." *Synthetic Metals*, **162**, 1954-1960.
- Veerender, P., Saxena, V., Jha, P., Koiry, S.P., Gusain, A., Samanta, S., Chauhan, A.K., Aswal, D.K., and Gupta, S.K. (2012). "Free-standing polypyrrole films as substrate-free and Pt-free counter electrodes for quasi-solid dye-sensitized solar cells." *Organic Electronics*, **13**, 3032-3039.
- Vijayakumar, P., Senthil Pandian, M., Pandikumar, A. and Ramasamy P. (2017). "A facile one-step synthesis and fabrication of hexagonal palladium-carbon nanocubes (H-Pd/C NCs) and their application as an efficient counter electrode for dye-sensitized solar cell (DSSC)." *Ceramics International*, **43**, 8466-8474.
- Wang, G., Yan, C., Hou, S., and Zhang, W. (2017). "Low-cost counter electrodes based on nitrogen-doped porous carbon nanorods for dye-sensitized solar cells." *Materials Science in Semiconductor Processing*, **63**, 190-195.
- Xia, J., Chen L., and Yanagida, S. (2011). "Application of polypyrrole as a counter electrode for a dye-sensitized solar cell." *Journal of Materials Chemistry*, **21**, 4644-4649.
- Yeh, M.H., Lee, C.P., Lin, L.Y., Nien, P.C., Chen, P.Y., Vittal, R., and Ho, K.C. (2011). "A composite poly(3,3-diethyl-3,4-dihydro-2H-thieno-[3,4-b][1,4]-dioxepine) and Pt film as a counter electrode catalyst in dye-sensitized solar cells."

- Electrochimica Acta*, **56**, 6157-6164.
- Yuan, H., Liu, J., Jiao, Q., Li, Y., Liu, X., Shi, D., Wu, Q., Zhao, Y., and Li, H. (2017). “Sandwich-like octahedral cobalt disulfide/reduced graphene oxide as an efficient Pt-free electrocatalyst for high-performance dye-sensitized solar cells.” *Carbon*, **119**, 225-234.
- Yue, G., Yang, G., Li, F., and Wu, J. (2015). “PEDOT:PSS assisted preparation of a graphene/nickel cobalt oxide hybrid counter electrode to serve in efficient dye-sensitized solar cells.” *RSC Advances*, **5**, 100159-100168.
- Zhang, J., Hreid, T., Li, X., Guo, W., Wang, L., Shi, X., Su, H., and Yuan, Z. (2010). “Nanostructured polyaniline counter electrode for dye-sensitised solar cells: Fabrication and investigation of its electrochemical formation mechanism.” *Electrochimica Acta*, **55**, 3664-3668.
- Zhou, Z., Sigdel, S., Gong, J., Vaagensmith, B., Elbohy, H., Yang, H., Krishnan, S., Wu, X.F., and Qiao, Q. (2016). “Graphene-beaded carbon nanofibers with incorporated Ni nanoparticles as efficient counter-electrode for dye-sensitized solar cells.” *Nano Energy*, **22**, 558-563.